Acta Oceanol. Sin., 2024, Vol. 43, No. 11, P. 1–11
https://doi.org/10.1007/s13131-024-2432-6
http://www.aosocean.com
E-mail: ocean2@hyxb.org.cn

An inner shelf penetrating front and its potential biogeochemical effects in the East China Sea during October

Hui Ding[1], Qinsheng Wei[1, 2*], Ming Xin[1], Yuhang Zhao[1], Bin Zhao[1], Mingyu Wang[1], Fei Teng[3], Xuehai Liu[3], Baodong Wang[1, 2*]

[1] Research Center for Marine Ecology, First Institute of Oceanography, Ministry of Natural Resources, Qingdao 266061, China

[2] Laboratory for Marine Ecology and Environmental Science, Qingdao Marine Science and Technology Center, Qingdao 266237, China

[3] Key Laboratory of Marine Environmental Science and Numerical Modeling, First Institute of Oceanography, Ministry of Natural Resources, Qingdao 266061, China

Received 21 December 2023; accepted 5 February 2024

Abstract

Based on *in-situ* observations in the East China Sea (ECS) during October 2021, we investigated a cross-shelf penetrating front (PF) in the inner shelf and explored its potential biogeochemical-ecological effects from a multidisciplinary perspective. The results show that a pronounced tongue-shaped PF was present at the southeast of the Hangzhou Bay, with salinity of 29–32 and a seaward horizontal penetration scale of ~200 km. It mainly occurred in the upper layers, and a spatial separation existed between this PF and the bottom salinity front in the northern coastal region off Zhejiang. In contrast, the salinity fronts at surface and bottom were well matched in the southern coastal area. Compared to the surface-to-bottom consistent coastal front in the southern region off Zhejiang, a stronger thermocline and halocline were sustained in the northern PF-dominated region, and suitable conditions could be achieved for phytoplankton growth and accumulation. The *in-situ* observed high-chlorophyll *a* (Chl *a*) zone in a seaward tongue shape was further an important indicator or signal for PF occurrence, and it was responsible for the decoupling of nutrient distributions and PF. The southern coastal front off Zhejiang might largely restrict the seaward transport of nutrients, and the dynamic environment under weak stratification in this region was disadvantageous for the growth of phytoplankton; thus the Chl *a* content was maintained at a relatively low level near the southern coastal region. Our results demonstrate that the PF combined with the coastal front may play an important role in shaping/regulating hydrodynamics, nutrient distributions and the Chl *a* regime over the inner ECS shelf.

Key words: penetrating front, biogeochemical effects, nutrient, chlorophyll *a*, East China Sea

Citation: Ding Hui, Wei Qinsheng, Xin Ming, Zhao Yuhang, Zhao Bin, Wang Mingyu, Teng Fei, Liu Xuehai, Wang Baodong. 2024. An inner shelf penetrating front and its potential biogeochemical effects in the East China Sea during October. Acta Oceanologica Sinica, 43(11): 1–11, doi: 10.1007/s13131-024-2432-6

1 Introduction

As the boundaries or interfaces between different water masses, the oceanic front is a highly dynamic zone with sharp gradients in various environmental variables (Belkin et al., 2009). The front usually occurs on multiple scales. Spatially, it may range from a few meters up to thousands of kilometers; temporally, the front may be short-lived (days) quasi-stationary, seasonally persistent or prominent (Belkin et al., 2009; Wang et al., 2015, 2021). Oceanic fronts are extremely involved in physical-biogeochemical interactions, playing an important role in regulating hydrodynamics, material transport and associated biogeochemical-ecological processes (Huang et al., 2010; Wang et al., 2013; Woodson and Litvin, 2015; Liu et al., 2018; Wei et al., 2016, 2020, 2022; Belkin, 2021; Li et al., 2021b; Lv et al., 2022). In recent decades, with enhanced observations and the widespread use of satellite-derived remote sensing data, oceanic fronts have attracted increasing attention.

The East China Sea (ECS) (Fig. 1), which is mainly surrounded by the Chinese mainland and Taiwan Island, Ryūkyū Islands and Kyūshū, is a productive marginal sea of the Northwest Pacific Ocean (Chen and Chen, 2003; Gong et al., 2003). The ECS shelf is significantly affected by coastal and open sea current systems (Yuan and Hsueh, 2010; Zhou et al., 2015; Liu et al., 2021)(Fig. 1), which can largely drive the physical-biogeochemical-ecological processes in this marginal sea (Liu et al., 2019; Wang and Wang, 2007; Wei et al., 2021b; Wang et al., 2023). Specifically, in the northern part of the ECS, Changjiang (Yangtze) Diluted Water (CDW) (Mao et al., 1963; Beardsley et al., 1985; Wu et al., 2014) prevails and changes seasonally in terms of direction. It generally flows northeastward during summer but turns southwestward when northerly wind rises in autumn. In the west, the Zhejiang-Fujian Coastal Current (ZFCC), which is mainly formed by the convergence of coastal seawater and runoff from multiple rivers (such as the Changjiang River, Qiantang River, Minjiang River, etc), flows southward along the coastline in wintertime and northward in summertime (Su, 2005; Zeng et al., 2012; Xu et al.,

Foundation item: The National Natural Science Foundation of China under contract Nos U23A2033 and 41876085; the Basic Scientific Fund of the National Public Research Institutes of China under contract No. 2020S03.
*Corresponding author, E-mail: weiqinsheng@fio.org.cn; wangbd@fio.org.cn

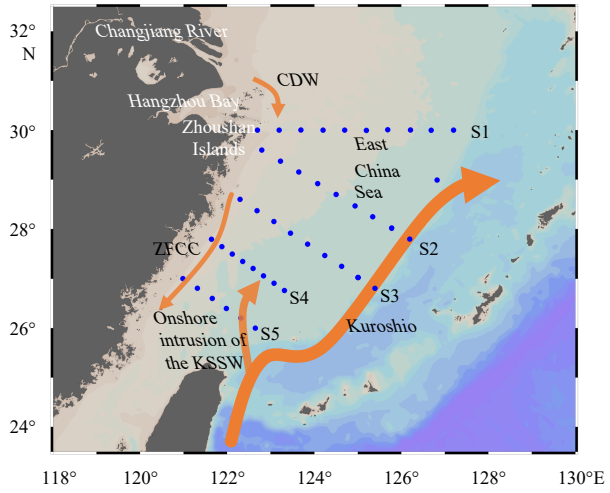

Fig. 1. Survey area and stations in the ECS during October 2021. Orange arrows generally denote the following main currents: Changjiang Diluted Water (CDW); Zhejiang-Fujian Coastal Current (ZFCC), Kuroshio and onshore intruded Kuroshio Subsurface Water (KSSW).

2015). In the east, the ECS is mainly under the stress of the Kuroshio (Hsueh, 2010; Wang and Oey, 2016), which carries high salinity water to the ECS and even interacts with the shelf currents. Notably, the Kuroshio Subsurface Water (KSSW) can be upwelled off northeast Taiwan and intrude northwestward to the inner ECS shelf (Yang et al., 2012; Xu et al., 2018; Cui et al., 2021). The above mentioned hydrodynamics provide favorable conditions for the formation of fronts in the ECS, including the Changjiang River plume front (Tian et al., 1993; Lie et al., 2003; Li et al., 2022), inshore front off the Zhejiang-Fujian coast (Pan et al., 1987; Tang and Zheng, 1990; Tang, 1996; Ning et al., 1998; Hickox et al., 2000; Lee et al., 2015; He et al., 2016; Cao et al., 2021; Belkin et al., 2023), and offshore front related to the Kuroshio (Guo and Ge, 1997; Park and Chu, 2006; Chang et al., 2008; Chen, 2009; Zhao et al., 2022; Belkin et al., 2023). These fronts are much more stable and present to be seasonally persistent or quasi-stationary year-round. Notably, Yuan et al. (2005) reported an intermittent cross-shelf penetrating front (PF) in the inner ECS shelf. Thereafter, some studies have addressed this phenomenon, primarily examining its possible mechanisms, including wind (He et al., 2010; Xuan et al., 2017; Bai, 2018; Ye et al., 2022; Zhou and Wu, 2023), frontal instability (Yuan et al., 2010), tide (Wu, 2015; Bai, 2018), barotropic pressure (Bai, 2018) and buoyant coastal currents (Zhou and Wu, 2023). The PF in the inner ECS shelf has strong seasonal-to-interannual variations, primarily occurring in summer and winter with a durative time from a few days to a month (He et al., 2010); moreover, it can cover a distance exceeding ~50 km or 100 km over the ECS shelf (He et al., 2010; Yuan et al., 2010). Notably, due to difficulties in PF observations, these studies were mainly based on satellite images of chlorophyll *a* (Chl *a*) and/or numerical models/experiments. And there is a lack of multidisciplinary analyses from an *in-situ* observational viewpoint. Currently, although some efforts have been devoted to the identification and mechanisms of PF in the inner ECS shelf, the associated biogeochemical-ecological processes in the PF-influenced region and its adjacent area have yet to be fully examined, especially based on *in-situ* observational data.

In this study, mainly based on *in-situ* observations in the ECS during autumn 2021, we attempt to identify an inner shelf PF and explore its potential biogeochemical-ecological effects. The results may deepen our understanding of PF in the ECS and provide insight into the roles of PF in regulating regional oceanographic processes.

2 Materials and methods

The investigation was conducted onboard the R/V *Xiangyanghong No. 18* during October 13–26, 2021. The cruise generally covered the region from the outside of Zhoushan Islands to the northern part of the Taiwan Strait, including 43 stations (Fig. 1). In terms of observational sections, the latitude of 30°N (generally from 122.5°E to 127.25°E) was chosen as Section S1; moreover, four sections (namely, from S2 to S5), which are basically perpendicular to the coastline, were designed parallel from north to south off Zhejiang (Fig. 1).

The hydrological parameters of temperature and salinity were determined using SBE-911. At each station, samples of nutrients and Chl *a* were collected according to regular water-sampling layers of surface (i.e., 2 m layer), 20 m, 30 m and bottom (i.e., ~2 m above the seabed). Nutrient samples were filtered by a 0.45 μm cellulose acetate membrane on board and preserved using polypropylene bottles in an about –20°C environment. They were analyzed in a land laboratory using an automatic nutrient analyzer (QuAAtro 39, SEAL Analytical GmbH, Germany). Specifically, nitrite nitrate, ammonia, phosphate and silicate were determined by diazo azo spectrophotometry, copper cadmium reduction, sodium hypobromite oxidation, phosphomolybdate blue spectrophotometry, and silomolybdate blue spectrophotomhetry, respectively; their detection limits were 0.02 μmol/L, 0.02 μmol/L, 0.04 μmol/L, 0.03 μmol/L and 0.25 μmol/L, respectively. The concentration of dissolved inorganic nitrogen (DIN) is the sum of the nitrite, nitrate and ammonia concentrations. Water samples of Chl *a* were filtered through Whatman GF/F filters on board, and the filters were folded and wrapped in aluminum foil and stored in liquid nitrogen until analysis. During laboratory measurement, the Chl *a* sample was first extracted with 90% acetone under low temperature and dark conditions for 24 hours. Then, its content was measured using a Trilogy fluorescence meter (Turner Designs, USA).

Moreover, the wind speeds during the investigation period were used in this study, which are the scatterometer vectors from the SeaWinds instrument onboard the QuikScat satellite. The data were averaged into mean-state vectors and subsetted into a one-half degree resolution for better visualization, as adopted by Yuan et al. (2005) and He et al. (2010). Jet Propulsion Laboratory Soil Moisture Active Passive (SMAP) Level 3 Sea Surface Salinity (SSS) 8-day running mean (http://apdrc.soest.hawaii.edu:80/dods/public_data/PODAAC/smap_local/jpl_v5.0/8day_running) was also used to obtain the averaged SSS regime during the cruise in the ECS. The SSS data are gridded at 0.25° × 0.25°, and a detailed description on the data acquisition can be found in Fore et al. (2016, 2020).

3 Results

3.1 *Hydrographic characteristics*

The horizontal distributions of temperature and salinity in the ECS during October 2021 are shown in Fig. 2. Overall, the temperature decreased from surface to bottom (Figs 2a–e); in contrast, the salinity exhibited an increasing trend downward (Figs 2f–j). Moreover, the salinity varied from low near the shore to high offshore, and a salinity front generally formed between the nearshore low-salinity water and the offshore saline water. Notably, a low-salinity water mass (salinity < 32) located at the

southeast of Hangzhou Bay, extended offshore near Section S2 in surface and 10 m layers (Figs 2f and g), which was forming a seaward tongue-shaped salinity front. Meanwhile, surface high-salinity water (>33) occurred in the southwest of the study area (Fig. 2f). In the layers below 10 m (Figs 2g–j), this high-salinity water intruded northeastward on a large scale from the southeastern ECS and even occupied the entire area outside the inner shelf. In addition, this saline water was also characterized by a

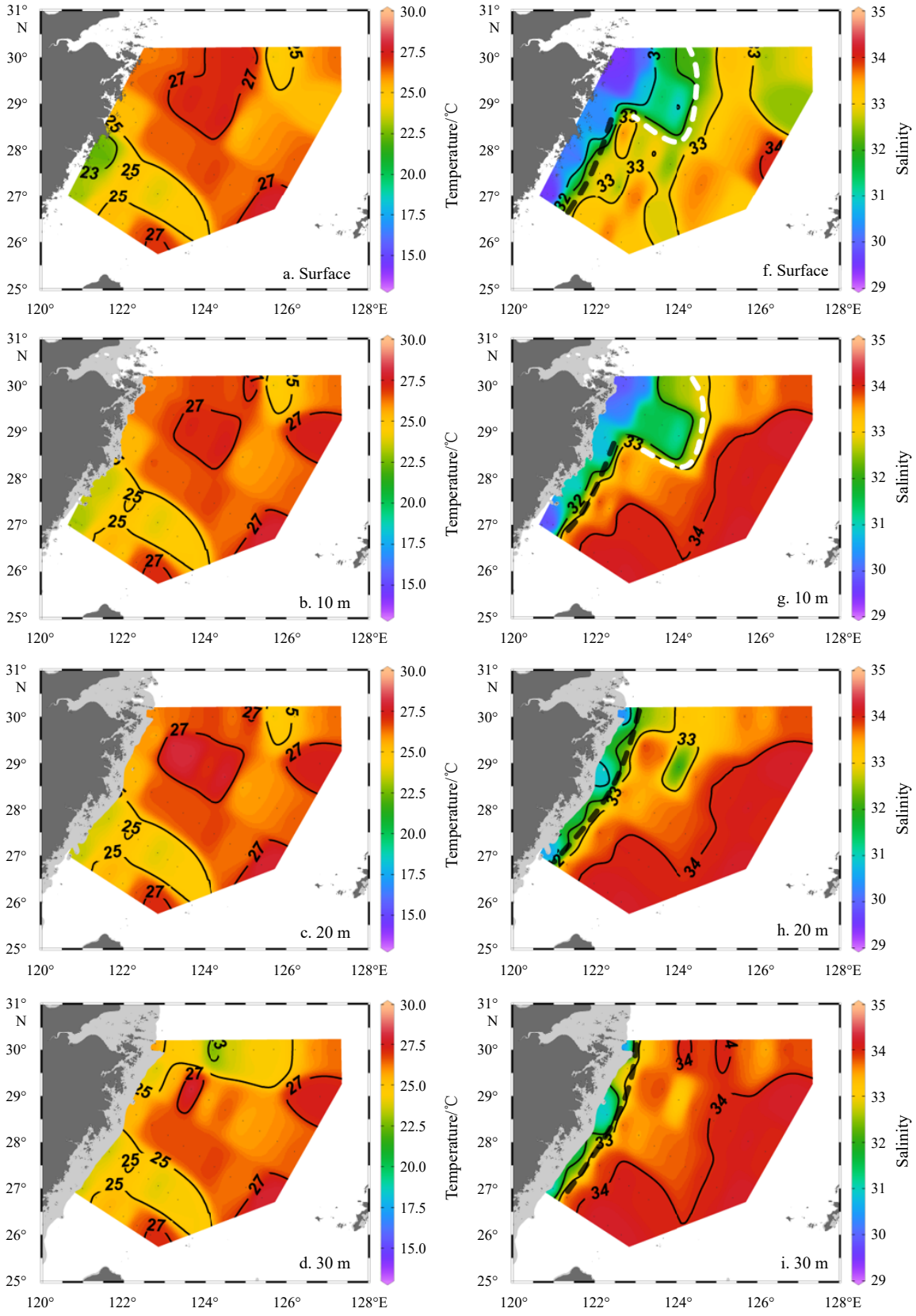

Fig. 2.

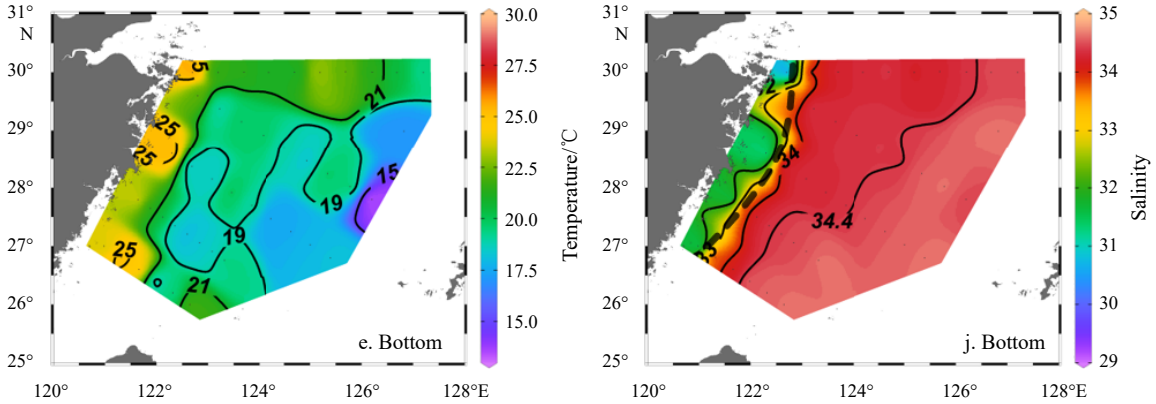

Fig. 2. Horizontal distributions of temperature (℃) and salinity in the ECS. The tongue-shaped white dashed line and the dark gray dashed line generally indicate the PF and coastal salinity front, respectively.

low temperature at bottom (Fig. 2e).

Vertically, the water column was generally stratified at each section (Fig. 3), with a thermocline and halocline occurring at subsurface, below which was a saline and low-temperature water mass. Remarkably, the seaward extension of low-salinity water was observed in the upper layers of the inner ECS shelf, especially along Sections S1 and S2 (Figs 3f and g). In addition, the cold and saline bottom water, which was mainly concentrated in the steep area along each section, tended to be uplifted onshore (Fig. 3). Influenced by the offshore extension of nearshore low-salinity water and onshore intrusion of saline bottom water, a dominant salinity front formed with its upper part inclining seaward, especially along Sections S1 and S2 (Figs 3f and g).

3.2 *Nutrient distributions*

Figs 4a–l show the horizontal distributions of nutrients in the ECS. Overall, nutrient concentrations generally increased from surface to bottom. They were relatively high off the Zhejiang coast in surface (Figs 4a, e and i) and 20 m (Figs 4b, f and j) layers, forming a dominant nutrient front. In 30 m layer (Figs 4c, g and k), high nutrient concentrations were observed in the northwestern region of the study area. Notably, a low-nutrient region extended from the northeast of Taiwan to the northwest in the upper layers (i.e., surface, 20 m and 30 m layers), which approximately corresponded to the northwestward saline water (Figs 4f–j). At bottom (Figs 4a, e and i), nutrient concentrations were high in the middle shelf and the southeastern ECS. The vertical distributions of nutrients along each section were similar (Figs 5a–o). In general, nutrient concentrations were relatively low in the upper layers and increased downward, especially in the offshore region of each section; high-nutrient areas formed in the bottom steep area along each section. A dominant nutricline existed at each section, and its location was roughly uplifted shoreward. Notably, upper-layer nutrients were greatly depleted in the nearshore region of Sections S1 and S2, while they were maintained at a high level in the coastal area of Sections S3, S4 and S5. Moreover, nutrient concentrations presented a downward decreasing trend in the nearshore region of Sections S4 and S5 (Figs 5d and e, i and j, n and o). This phenomenon well corresponded to the vertical distributions of salinity, which exhibited an increasing trend from surface to bottom (Figs 3i and j). These results indicate that the nutrients in this region mainly originated from the transport of coastal low-salinity water.

3.3 *Chl a patterns*

Figures 4m-p show the horizontal distributions of Chl *a* in the ECS. Overall, Chl *a* content decreased from surface to bottom. A high-Chl *a* region was observed at surface in the northwestern part of the study area, generally extending seaward along the Section S2 and forming a seaward tongue-shaped Chl *a* front (Fig. 4m). This high-Chl *a* region was in accordance with the low-salinity area southeast of Hangzhou Bay (Fig. 2f). Chl *a* content in the southeastern part of the study area was relatively low, roughly corresponding to the offshore saline water-influenced region (Fig. 2f) with low nutrients (Figs 4a, e and i). As shown by the vertical distributions of Chl *a* (Figs 5p–t), high Chl *a* content mainly formed in the upper layers in the nearshore region of Sections S1 and S2, presenting a tongue-shaped distribution from the coast to offshore (Figs 5p and q). In contrast, Chl *a* content was low in the coastal area of Sections S3, S4 and S5 (Figs 5r–t). In the offshore region of each section, Chl *a* content was maintained at a relatively low level and gradually decreased downward.

4 Discussion

4.1 *Water masses and their nutrient properties in the ECS during October*

During the period of investigation, the northwesterly wind began to prevail in the study area, as indicated by Fig. 6a. Subsequently, the low-salinity coastal water in the inner ECS shelf tended to spread southward along the coast of Zhejiang, as indicated by Figs 2f and g. It was mainly composed of the southward CDW (Mao et al., 1963; Beardsley et al., 1985) and the local ZFCC (Zeng et al., 2012). The offshore saline water, which extended northwestward from the southeastern ECS, denoted the influence of the Kuroshio (Hsueh, 2000; Yang et al., 2012; Qi et al., 2014). In particular, the upper-layer saline water with high temperature (Figs 2a–d, f–i) and bottom saline water with low temperature (Figs 2e and j) imply ECS shelf water and onshore intrusion of the KSSW (Yang et al., 2012; Xu et al., 2018; Cui et al., 2021), respectively. The ECS shelf water is mainly composed of the Kuroshio Surface Water (KSW)—originated saline water and the northward Taiwan Warm Current Water (Qi et al., 2014; Lian et al., 2016; Li et al., 2021a). Based on the temperature-salinity scatter plot (Fig. 6b), water masses could be further identified in the ECS.

The above-mentioned hydrographic conditions largely regulated the nutrient distributions. Generally, influenced by the southward extension of low-salinity coastal water (mainly from the ZFCC transport) (Figs 2f and g), a relatively high-nutrient zone formed in the surface (Figs 4a, e and i) and 20 m (Figs 4b, f

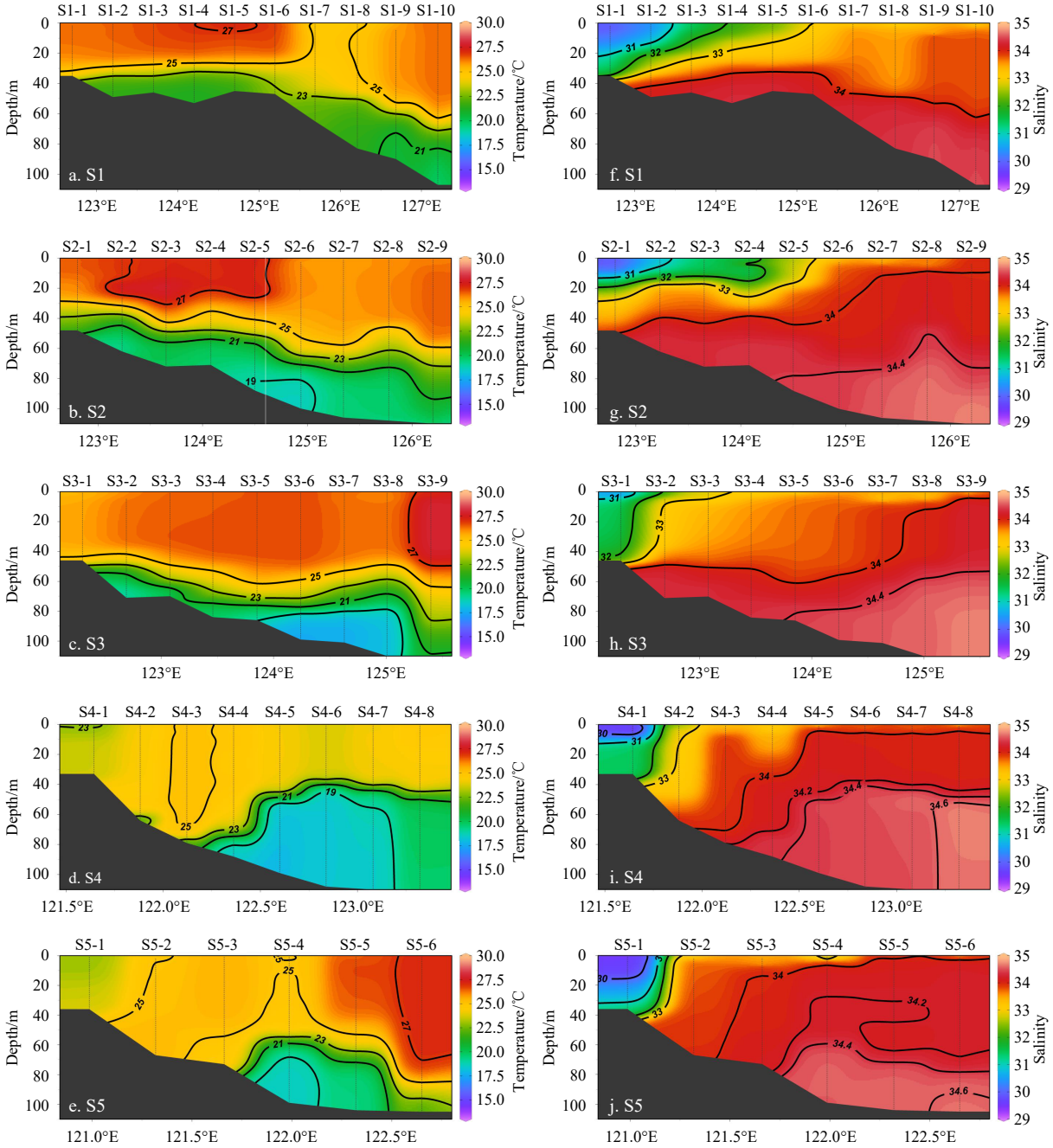

Fig. 3. Vertical distributions of temperature (℃) and salinity along sections from S1 to S5.

and j) layers in the southern nearshore region of the study area. Due to the oligotrophic ECS shelf water, the offshore surface region was characterized by low nutrients (Figs 4a, e and i). Partially caused by the northwestern intrusion of the KSSW, nutrients were maintained at a high level in the offshore bottom water (Figs 4d, h and l), especially for phosphate (Fig. 4h). Previous studies have revealed that the onshore branch of the KSSW can deliver a large amount of nutrients into the ECS shelf (Chen, 1996; Yang et al., 2013; Xu et al., 2020; Wang et al., 2018, 2023). Our results show that the highest nutrients were mainly concentrated in the bottom layer of the middle ECS shelf. Actually, the core of this high-nutrient region was roughly in accordance with the well-known summertime hypoxic zone in the ECS (Chen et al., 2007; Wei et al., 2017). We believe that in addition to originating from KSSW transport, the release from local mineralization of organic matter in the hypoxic zone might also contribute to the nutrient levels in this region, as also revealed by Zhu et al. (2017) and Wei et al. (2017, 2021b). Moreover, stratification (Fig. 3) could greatly hinder the vertical transport of nutrients and thus play a role in maintaining high nutrient levels in the bottom layer of the middle ECS shelf.

4.2 *PF in the inner ECS shelf*

Previously, the PF was found to be one of the most important physical processes in the inner ECS shelf (Yuan et al., 2005, 2010; He et al., 2010; Wu, 2015; Ye et al., 2022; Zhou and Wu, 2023). As indicated in Figs 2f and g, the tongue-shaped low salinity water, which mainly extended offshore in the upper layers (i.e., surface and 10 m layers) in the northwestern region of the study area, clearly suggests the existence of a cross-shelf PF in the ECS. Actu-

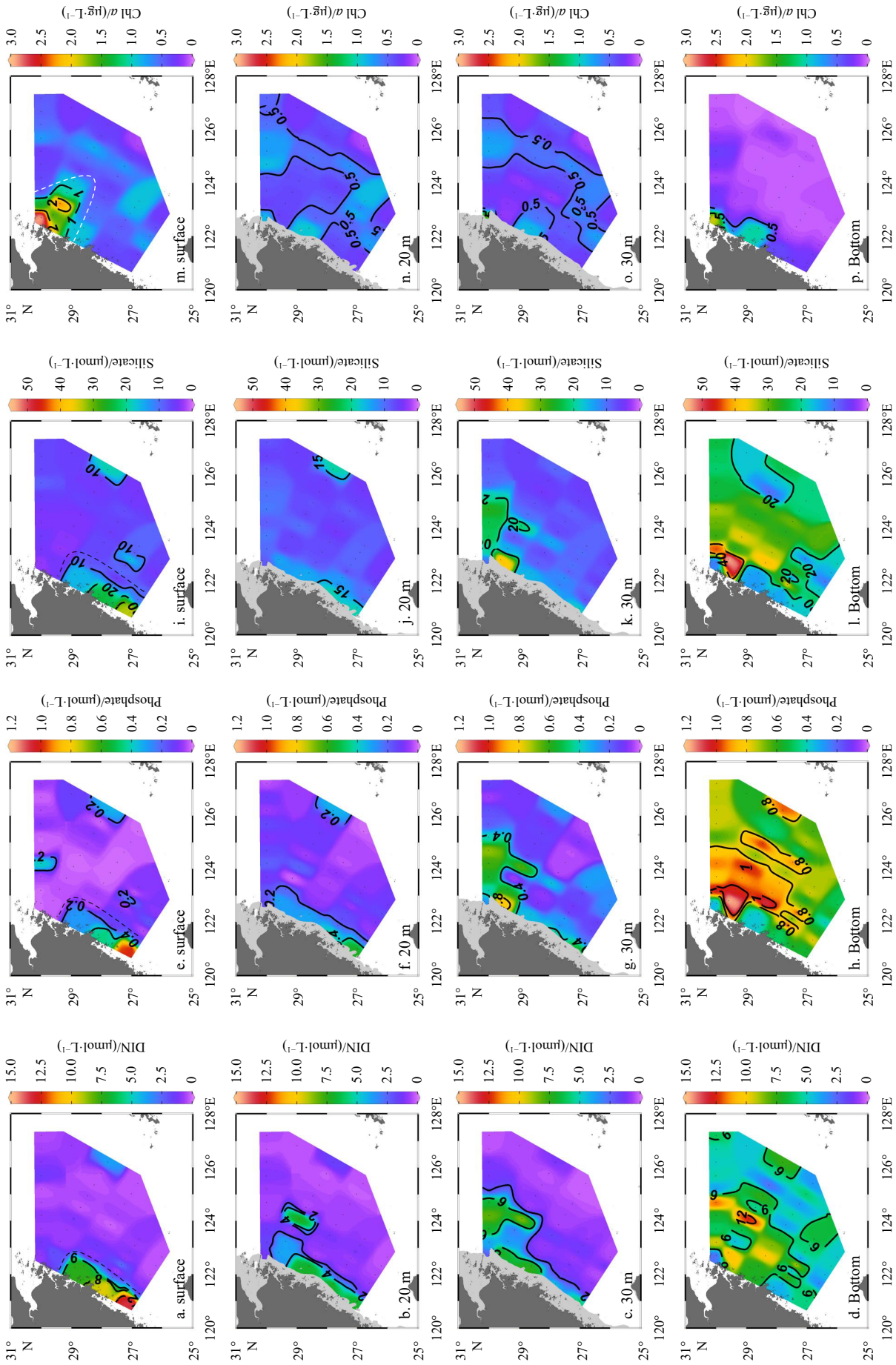

Fig. 4. Horizontal distributions of nutrients concentration (μmol/L) and Chl *a* content (μg/L) in the ECS. The gray dashed line (in Panels a, e and i) and tongue-shaped white dashed line (in Panel m) indicate the nutrient front and Chl *a* front, respectively.

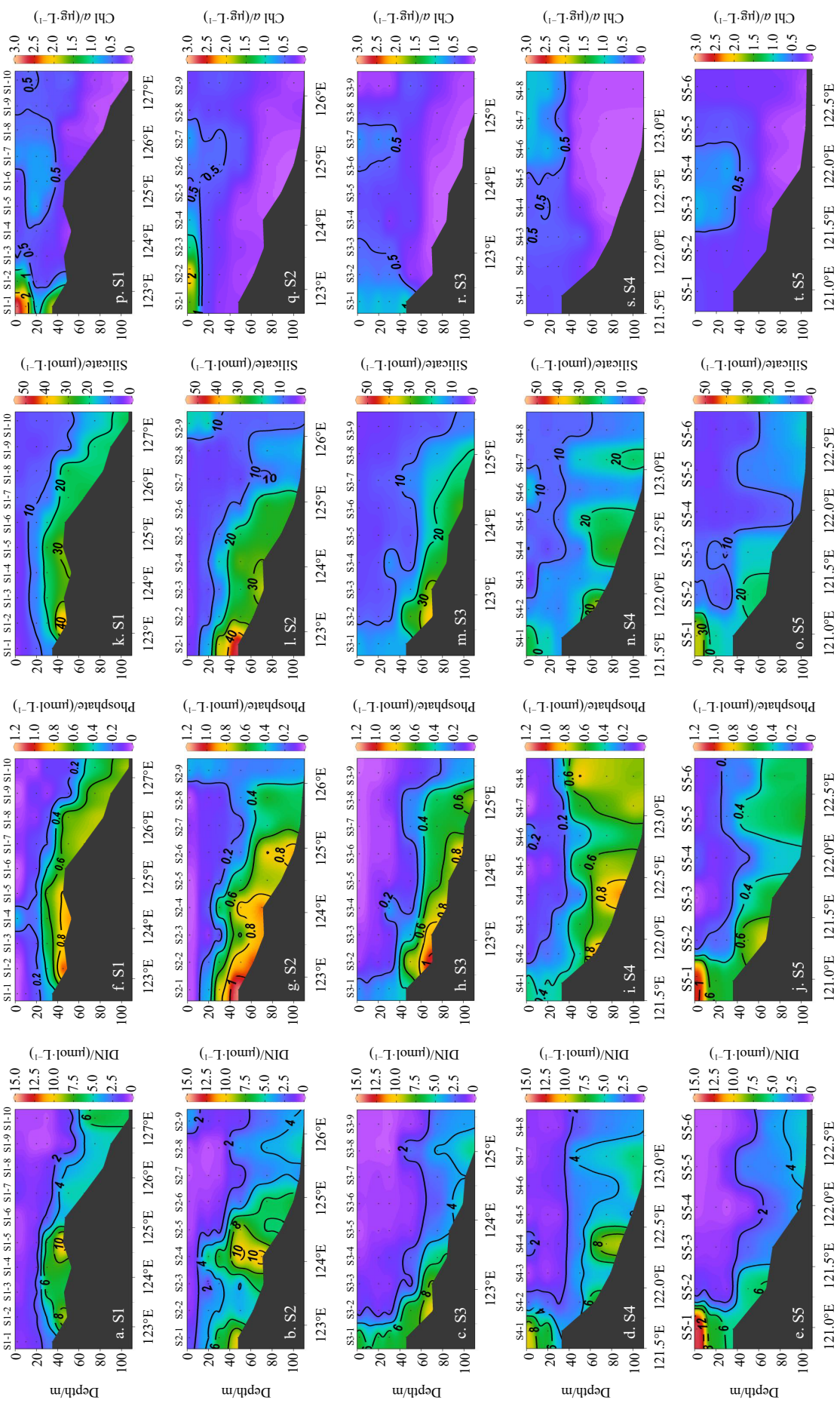

Fig. 5. Vertical distributions of nutrients concentration (μmol/L) and Chl *a* content (μg/L) along sections from S1 to S5.

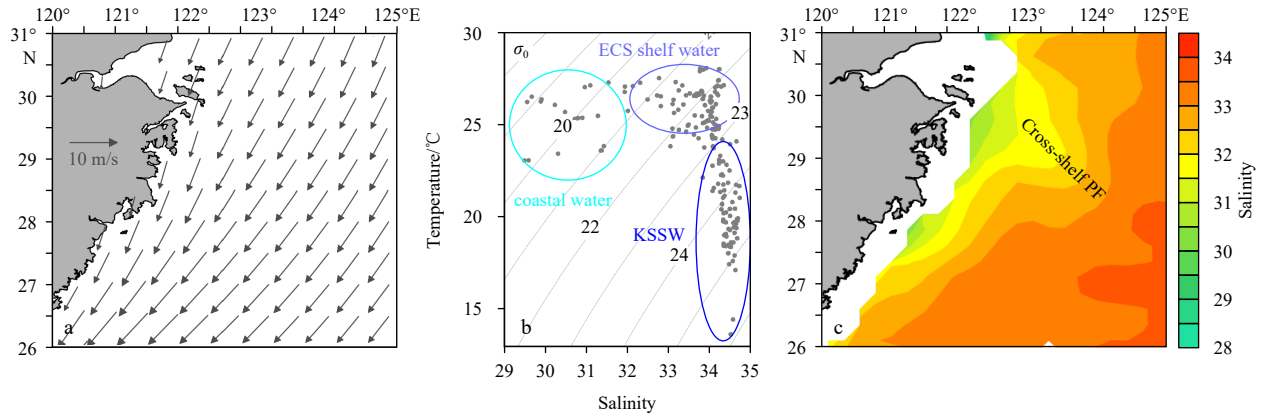

Fig. 6. Averaged wind field during the cruise (a), temperature-salinity scatter plot (b) and satellite-derived SSS (c) in the ECS.

ally, the seaward extension of low-salinity water along Sections S1 and S2 (Figs 3f and g) could further confirm the occurrence of PF. In addition, the distribution of satellite-derived mean SSS during the cruise also indicates the occurrence of PF in the ECS shelf (Fig. 6c). Overall, this cross-shelf PF generally covered a large distance from the coast, resulting in an offshore intrusion into the middle shelf. The salinity of this penetrated water was mainly between 29 and 32 (Figs 2f and g), and the horizontal penetration scale of PF could reach ~200 km from the coast, which was comparable to the satellite-derived results of He et al. (2010). The analyses on the variability in PF revealed that it was mainly observed during summer and winter in the inner ECS shelf (He et al., 2010). Here, our results confirmed that the PF could occur in autumn, as also illustrated by Zhou and Wu. (2023). The PF location was approximately southeast of Hangzhou Bay (Figs 2f and g), generally penetrating offshore near the Zhoushan Islands. The formation of PF is largely due to complicated hydrodynamics (He et al., 2010; Yuan et al., 2010; Wu, 2015; Ye et al., 2022; Zhou and Wu, 2023), among which the accumulation of southward-transported coastal water under favorable wind conditions is one of the most important factors. The northwesterly wind (Fig. 6a) during the cruise was conducive to the southeastward extension of the coastal diluted waters (Figs 2f and g). Moreover, these inshore waters tended to be transported eastward when encountering the northward saline ECS shelf water off Zhejiang. The relatively sharp salinity gradients between the PF-dominated region and the saline seawater to the southeast partially implied their interactions (Figs 2f and g). In addition, the curved headlands near the Zhoushan Islands could also favor the offshore penetration of coastal water plumes (Zhou and Wu, 2023).

In the southern nearshore region off Zhejiang, forced by the shoreward Kuroshio water, the inshore diluted water was mainly trapped along the coast and thus a coastal salinity front formed (Figs 2f–j). This coastal front was connected to the nearshore part of the PF near 29°N in the surface and 10 m layers (Figs 2f and g). Notably, the cross-shelf PF mainly occurred in the upper layers in the north, while the coastal salinity front could be maintained from surface to bottom in the south and extend to the northern region along the shorelines (Figs 2f–j). As a result, a spatial separation existed between the upper-layer PF and bottom salinity front in the northwestern region of the study area. In contrast, the surface and bottom salinity fronts were well matched with each other in the southern coastal region. Moreover, our observations show that the saline KSSW could reach the shore much closer in the northern PF-dominated region than in the south, as indicated by 23℃ isotherm and 34 isohaline in the vertical distributions of temperature and salinity along Sections from S1 to S5 (Fig. 3). Influenced by the seaward PF in upper layers and the more shoreward intrusion of the KSSW at bottom, a stronger thermocline and halocline could be achieved in the northwestern region of the study area (i.e., the nearshore of Sections S1 and S2), as implied by the vertical distributions of temperature and salinity along Sections S1 and S2 (Figs 3a and b, f and g). However, in the southwestern region of study area (i.e., the southern coastal area off Zhejiang), stratification was greatly weakened, and the water column tended to be vertically mixed, especially in the nearshore region of Sections S4 and S5 (Figs 3d, e, i and j).

4.3 *Potential biogeochemical-ecological effects of PF*

Fronts are among the most important physical processes and may play an important role in the transport and exchange of substances (Li et al., 2003; Dong et al., 2011; Ren et al., 2015; Wei et al., 2020). Undoubtedly, the unique PF in the ECS could drive the delivery of seawater from the inner shelf to the middle shelf, thus enhancing material exchange and influencing regional biogeochemical-ecological processes. In fact, the seaward extension of tongue-shaped low-salinity water (Figs 2f and g) should have a significant impact on the cross-shelf transport of nutrients under the influence of PF. However, in this PF-dominated area, nutrient concentrations were very low (Figs 4a, e and i), showing the decoupling of nutrient distributions and PF. This might be largely attributed to the biological consumption of phytoplankton, as indicated by the tongue-shaped high-Chl *a* zone (Fig. 4m). The relationship between Chl *a* and salinity in the surface layer (Fig. 7a) could further suggest phytoplankton blooms within the low-salinity PF-dominated region. Hence, the seaward-transported nutrients along with the cross-shelf PF were mainly depleted to support primary production, as implied by Fig. 7b. These results were responsible for the inconsistency of the PF (Fig. 2f) and nutrient distributions (Figs 4a, e and i). Actually, the significant stratification in the PF-dominated area (Figs 3a and b, f and g) was also conducive to the accumulation of phytoplankton in the upper layers (Fig. 4m and Figs 5p and q). Moreover, the settlement of suspended particulate matter (SPM) over a relatively long distance and period within the seaward PF-dominated region would considerably reduce the seawater turbidity, potentially improving the light transmission property. This was previously confirmed by Wei et al. (2021a), who demonstrated that the seaward surface plume front far from the coast favors the settlement of SPM and reduction of turbidity in the Changjiang River Estuary and adjacent areas. As a result, suitable conditions could be achieved for phytoplankton growth in the PF-dominated area, and the *in-situ* observed high-Chl *a* zone in a seaward tongue

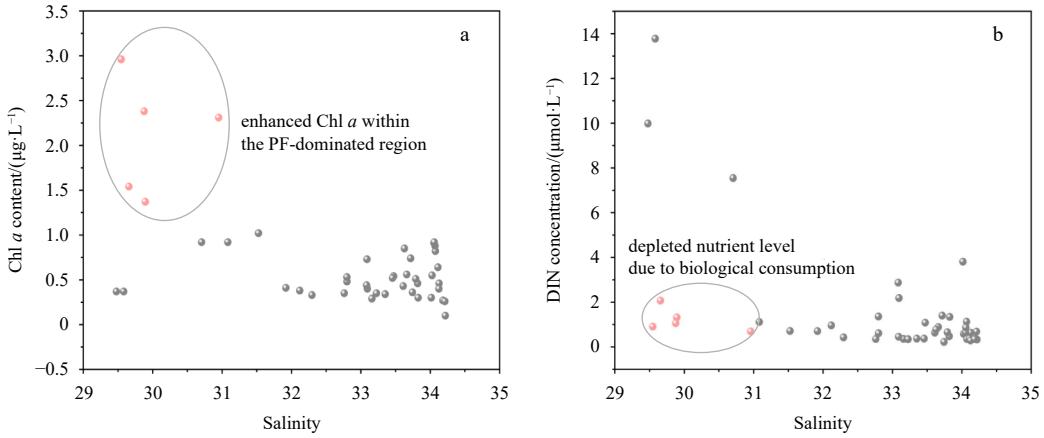

Fig. 7. Relationships between the related variables in the surface layer. a. Chl *a* and salinity; b. DIN and salinity. The red dots indicate the sites with high Chl *a* and low nutrients in the low-salinity PF-dominated region.

shape was a further significant indicator or signal of PF in the inner ECS shelf. Exactly, we believe that the nutrients depleted by phytoplankton within the PF-dominated region (Fig. 7b) were mainly from the southward CDW and ZFCC, as suggested by low-salinity water in Figs 2f and g. Here, quantitatively estimating the contribution of PF to nutrient transport is challenging because of the complex processes, which suggests the need of model constructing for physical-biogeochemical-ecological interactions in the future. In addition, the shoreward transport of nutrients along with the KSSW tended to be upwelled in the northern nearshore region, as indicated by Figs 5a, b, f, g, k and l. The high-nutrient area, which occurred in 30 m layer in the northwestern region of the study area (Figs 4c, g and k), further confirmed the upward transport of nutrients underneath the PF. This process might also play a role in supporting primary production when rapid nutrient consumption occurred in the PF-dominated upper layers (Figs 5a and b, f, g, k and l).

In contrast, the surface-to-bottom consistent coastal front in the southern region off Zhejiang (Figs 2f–j) might act as a barrier for the seaward transport of substances, as previously indicated by Liu et al. (2015) and Qiao et al. (2020). Thereby, the low-salinity water rich in nutrients was mainly trapped along the coast in this area (Figs 2f and g and Figs 4a, e and i). Moreover, the dynamic environment under much weaker stratification (Figs 3d and e) on the nearshore side of this southern coastal front was not conducive to the settlement of SPM. As a result, light transmission could greatly be reduced, potentially leading to poor light conditions for phytoplankton growth in upper layers. Actually, the vertical convection induced by the unstable dynamic environment in this area was also disadvantageous for the accumulation of phytoplankton. Therefore, a low Chl *a* content was observed near the southern coastal region off Zhejiang (Fig. 4m and Figs 5r–t). The weak phytoplankton production also meant low consumption of nutrients, which was in turn responsible for high nutrient concentrations in the southern coastal area off Zhejiang (Figs 4a, e and i). Consequently, the nutrients from the transport of the southward ZFCC could be maintained in the southern nearshore region. The aforementioned analyses demonstrate that the PF combined with the coastal front may play an important role in shaping/regulating hydrodynamics, nutrient distributions and the Chl *a* regime over the inner ECS shelf.

5 Conclusions

Using field observations in the ECS during October 2021, this study investigated a cross-shelf PF in the inner ECS shelf, and the potential biogeochemical-ecological effects of PF were explored by multidisciplinary analyses.

(1) A pronounced inner shelf PF was identified, and the salinity within this seaward-penetrated PF was mainly between 29 and 32. This front was approximately southeast of Hangzhou Bay, generally penetrating offshore near the Zhoushan Islands. It covered a large distance from the coast, with a horizontal penetration scale of ~200 km.

(2) The cross-shelf PF mainly occurred in the upper layers, and a spatial separation existed between the upper-layer PF and bottom salinity front in the northern coastal region of the study area. In contrast, the surface and bottom salinity fronts were well matched with each other in the southern coastal region off Zhejiang. Moreover, a stronger thermocline and halocline were maintained in the PF-dominated region.

(3) Suitable conditions could be achieved for phytoplankton growth in the PF-dominated area, and the *in-situ* observed high-Chl *a* zone in a seaward tongue shape was a significant indicator or signal of PF. The phytoplankton consumption was responsible for the decoupling of nutrient distributions and PF. The southern coastal front off Zhejiang might restrict the seaward transport of nutrients, and the dynamic environment under weak stratification in this region was disadvantageous for the growth and accumulation of phytoplankton; thus a low Chl *a* content was observed near the southern coastal region. The PF combined with the coastal front plays an important role in shaping/regulating nutrient distributions and the Chl *a* regime over the inner ECS shelf.

Acknowledgements

Data and samples of this research were collected onboard the R/V *Xiangyanghong No. 18* implementing the open research cruise NORC2021-02 supported by the NSFC Shiptime Sharing Project (project number: 42049902). We are grateful to the survey team and crew for their help and cooperation during the field investigation.

References

Bai Mei. 2018. Revealing the multiple-scale spatiotemporal variations of the Changjiang River plume by the self-organizing map (SOM) method (in Chinese)[dissertation]. Shanghai: East China Normal University

Beardsley R C, Limeburner R, Yu H, et al. 1985. Discharge of the Changjiang (Yangtze River) into the East China Sea. Continental Shelf Research, 4(1–2): 57–76, doi: 10.1016/0278-4343(85)

90022-6
Belkin I M. 2021. Remote sensing of ocean fronts in marine ecology and fisheries. Remote Sensing, 13(5): 883, doi: 10.3390/rs13050883
Belkin I M, Cornillon P C, Sherman K. 2009. Fronts in large marine ecosystems. Progress in Oceanography, 81(1–4): 223–236, doi: 10.1016/j.pocean.2009.04.015
Belkin I M, Lou Shangshang, Yin Wenbin. 2023. The China coastal front from *Himawari-8* AHI SST data-Part 1: East China Sea. Remote Sensing, 15(8): 2123, doi: 10.3390/rs15082123
Cao Lu, Tang Rui, Huang Wei, et al. 2021. Seasonal variability and dynamics of coastal sea surface temperature fronts in the East China Sea. Ocean Dynamics, 71(2): 237–249, doi: 10.1007/s10236-020-01427-8
Chang Y, Lee M A, Shimada T, et al. 2008. Wintertime high-resolution features of sea surface temperature and chlorophyll-α fields associated with oceanic fronts in the southern East China Sea. International Journal of Remote Sensing, 29(21): 6249–6261, doi: 10.1080/01431160802175462
Chen Chen-Tung Arthur. 1996. The Kuroshio intermediate water is the major source of nutrients on the East China Sea continental shelf. Oceanologica Acta, 19(5): 523–527
Chen Chen-Tung Arthur. 2009. Chemical and physical fronts in the Bohai, Yellow and East China Seas. Journal of Marine Systems, 78(3): 394–410, doi: 10.1016/j.jmarsys.2008.11.016
Chen Chen-Tung Arthur, Chen Houng-Yung. 2003. Nitrate-based new production and its relationship to primary production and chemical hydrography in spring and fall in the East China Sea. Deep-Sea Research Part II: Topical Studies in Oceanography, 50(6–7): 1249–1264
Chen Chung-Chi, Gong Gwo-Ching, Shiah F K. 2007. Hypoxia in the East China Sea: one of the largest coastal low-oxygen areas in the world. Marine Environmental Research, 64(4): 399–408, doi: 10.1016/j.marenvres.2007.01.007
Cui Xuan, Yang Dezhou, Sun Chaojiao, et al. 2021. New insight into the onshore intrusion of the Kuroshio into the East China Sea. Journal of Geophysical Research: Oceans, 126(2): e2020JC016248, doi: 10.1029/2020JC016248
Dong Lixian, Guan Weibing, Chen Qi, et al. 2011. Sediment transport in the Yellow Sea and East China Sea. Estuarine, Coastal and Shelf Science, 93(3): 248–258
Fore A G, Yueh S H, Tang W Q, et al. 2016. Combined active/passive retrievals of ocean vector wind and sea surface salinity with SMAP. IEEE Transactions on Geoscience and Remote Sensing, 54(12): 7396–7404
Fore A, Yueh S, Tang W, et al. 2020. JPL SMAP ocean surface salinity products [Level 2B, Level 3 Running 8-day, Level 3 Monthly], Version 5.0 validated release. Pasadena, CA, USA: Jet Propulsion Laboratory
Gong Gwo-Ching, Wen Yun-Ho, Wang Bowen, et al. 2003. Seasonal variation of chlorophyll *a* concentration, primary production and environmental conditions in the subtropical East China Sea. Deep-Sea Research Part II: Topical Studies in Oceanography, 50(6–7): 1219–1236, doi: 10.1016/S0967-0645(03)00019-5
Guo Binghuo, Ge Renfeng. 1997. Role of Kuroshio frontal eddy in exchange between shelf water and Kuroshio water in East China Sea. Acta Oceanologica Sinica, 16(1): 1–18
He Shuangyan, Huang Daji, Zeng Dingyong. 2016. Double SST fronts observed from MODIS data in the East China Sea off the Zhejiang–Fujian coast, China. Journal of Marine Systems, 154: 93–102, doi: 10.1016/j.jmarsys.2015.02.009
He Lei, Li Yao, Zhou Hui, et al. 2010. Variability of cross-shelf penetrating fronts in the East China Sea. Deep-Sea Research Part II: Topical Studies Oceanography, 57(19–20): 1820–1826
Hickox R, Belkin I, Cornillon P, et al. 2000. Climatology and seasonal variability of ocean fronts in the East China, Yellow and Bohai seas from satellite SST data. Geophysical Research Letters, 27(18): 2945–2948
Hsueh Y. 2000. The Kuroshio in the East China Sea. Journal of Marine Systems, 24(1–2): 131–139.
Huang Daji, Zhang Tao, Zhou Feng. 2010. Sea-surface temperature fronts in the Yellow and East China seas from TRMM microwave imager data. Deep-Sea Research Part II: Topical Studies in Oceanography, 57(11–12): 1017–1024
Lee Ming-an, Chang Yi, Shimada T. 2015. Seasonal evolution of fine-scale sea surface temperature fronts in the East China Sea. Deep Sea Research Part II: Topical Studies in Oceanography, 119: 20–29
Li Chunyan, Nelson J R, Koziana J V. 2003. Cross-shelf passage of coastal water transport at the South Atlantic Bight observed with MODIS Ocean Color/SST. Geophysical Research Letters, 30(5): 1257
Li Weiqi, Ge Jianzhong, Ding Pingxing, et al. 2021b. Effects of dual fronts on the spatial pattern of chlorophyll-*a* concentrations in and off the Changjiang River Estuary. Estuaries and Coasts, 44(5): 1408–1418, doi: 10.1007/s12237-020-00893-z
Li Shuangzhao, Zhang Zhaoru, Zhou Meng, et al. 2022. The role of fronts in horizontal transports of the Changjiang River plume in summer and the implications for phytoplankton blooms. Journal of Geophysical Research: Oceans, 127(8): e2022JC018541, doi: 10.1029/2022JC018541
Li Shuangzhao, Zhong Yisen, Zhou Meng, et al. 2021a. Mixed layer water mass analysis on the East China Sea inner shelf. Estuarine, Coastal and Shelf Science, 261: 107561
Lian Ergang, Yang Shouye, Wu Hui, et al. 2016. Kuroshio subsurface water feeds the wintertime Taiwan warm current on the inner East China Sea shelf. Journal of Geophysical Research: Oceans, 121(7): 4790–4803
Lie H J, Cho C H, Lee J H, et al. 2003. Structure and eastward extension of the Changjiang River plume in the East China Sea. Journal of Geophysical Research: Oceans, 108(C3): 3077
Liu Zhiqiang, Gan Jianping, Hu Jianyu, et al. 2021. Progress of studies on circulation dynamics in the East China Sea: The Kuroshio exchanges with the shelf currents. Frontiers in Marine Science, 8: 620910, doi: 10.3389/fmars.2021.620910
Liu Xin, Laws E A, Xie Yuyuan, et al. 2019. Uncoupling of seasonal variations between phytoplankton chlorophyll *a* and production in the East China Sea. Journal of Geophysical Research: Biogeosciences, 124(7): 2400–2415, doi: 10.1029/2018JG004924
Liu Shidong, Qiao Lulu, Li Guangxue, et al. 2015. Distribution and cross-front transport of suspended particulate matter over the inner shelf of the East China Sea. Continental Shelf Research, 107: 92–102, doi: 10.1016/j.csr.2015.07.013
Liu Dongyan, Wang Yanna, Wang Yueqi, et al. 2018. Ocean fronts construct spatial zonation in microfossil assemblages. Global Ecology and Biogeography, 27(10): 1225–1237, doi: 10.1111/geb.12779
Lv Ting, Liu Dongyan, Zhou Peng, et al. 2022. The coastal front modulates the timing and magnitude of spring phytoplankton bloom in the Yellow Sea. Water Research, 220: 118669.
Mao Hanlee, Kan Tze-Chun, Lan Shufang. 1963. A preliminary study of the Yangtze diluted water and its mixing processes. Haiyang Xuebao (in Chinese), 5(3): 183–206
Ning Xiuren, Liu Zilin, Cai Ying, et al. 1998. Physicobiological oceanographic remote sensing of the East China Sea: satellite and *in situ* observations. Journal of Geophysical Research: Oceans, 103(C10): 21623–21635, doi: 10.1029/98JC01612
Pan Yuqiu, Xu Duanrong, Xu Jianping. 1987. The structure of fronts and their causes in the coastal upwelling area off Zhejiang. Acta Oceanologica Sinica, 6(2): 177–189
Park S, Chu P C. 2006. Thermal and haline fronts in the Yellow/East China Seas: Surface and subsurface seasonality comparison. Journal of Oceanography, 62(5): 617–638
Qi Jifeng, Yin Baoshu, Zhang Qilong, et al. 2014. Analysis of seasonal variation of water masses in East China Sea. Chinese Journal of Oceanology and Limnology, 32(4): 958–971, doi: 10.1007/s00343-014-3269-1
Qiao Lulu, Liu Shidong, Xue Wenjing, et al. 2020. Spatiotemporal variations in suspended sediments over the inner shelf of the East China Sea with the effect of oceanic fronts. Estuarine, Coastal and Shelf Science, 234: 106600
Ren Jingling, Xuan Jiliang, Wang Zhaowei, et al. 2015. Cross-shelf transport of terrestrial Al enhanced by the transition of northeasterly to southwesterly monsoon wind over the East China

Sea. Journal of Geophysical Research: Oceans, 120(7): 5054–5073
Su Jilan. 2005. Hydrology in China Sea (in Chinese). Beijing: China Ocean Press
Tang Yuxiang. 1996. Distributional features and seasonal variations of temperature fronts in the East China Sea. Oceanologia et Limnologia Sinica (in Chinese), 27(4): 436–444
Tang Yuxiang, Zheng Yifang. 1990. Research on fronts in East China Sea. Marine Science Bulletin (in Chinese), 9(5): 89–96
Tian R C, Hu F X, Martin J M. 1993. Summer nutrient fronts in the Changjiang (Yangtze River) Estuary. Estuarine, Coastal and Shelf Science, 37(1): 27–41
Wang Baodong, Wang Xiulin. 2007. Chemical hydrography of coastal upwelling in the East China Sea. Chinese Journal of Oceanology and Limnology, 25(1): 16–26, doi: 10.1007/s00343-007-0016-x
Wang Jia, Oey L Y. 2016. Seasonal exchanges of the Kuroshio and shelf waters and their impacts on the shelf currents of the East China Sea. Journal of Physical Oceanography, 46(5): 1615–1632, doi: 10.1175/JPO-D-15-0183.1
Wang Yuntao, Castelao R M, Yuan Yeping. 2015. Seasonal variability of alongshore winds and sea surface temperature fronts in Eastern Boundary Current Systems. Journal Geophysical Research: Oceans, 120(3): 2385–2400, doi: 10.1002/2014JC010379
Wang Yichen, Chen Wenyu, Chang Yi, et al. 2013. Ichthyoplankton community associated with oceanic fronts in early winter on the continental shelf of the southern East China Sea. Journal of Marine Science and Technology, 21(7): 10
Wang Yuntao, Ma Wentao, Zhou Feng, et al. 2021. Frontal variability and its impact on chlorophyll in the Arabian Sea. Journal of Marine Systems, 218: 103545
Wang Wentao, Yu Zhiming, Song Xiuxian, et al. 2018. Intrusion pattern of the offshore Kuroshio Branch Current and its effects on nutrient contributions in the East China Sea. Journal of Geophysical Research: Oceans, 123(3): 2116–2128, doi: 10.1002/2017JC013538
Wang Wentao, Yu Zhiming, Song Xiuxian, et al. 2023. Nitrate dynamics and source apportionment on the East China Sea shelf revealed by nitrate stable isotopes and a Bayesian mixing model. Science of the Total Environment, 869: 161762, doi: 10.1016/j.scitotenv.2023.161762
Wei Qinsheng, Fu Mingzhu, Li Xiansen, et al. 2022. Front-driven physical–biogeochemical–ecological interactions in the Yellow Sea large marine ecosystem. In: Belkin I M, ed. Chemical Oceanography of Frontal Zones. Berlin, Heidelberg: Springer
Wei Qinsheng, Fu Mingzhu, Sun Junchuan, et al. 2020. Seasonal physical fronts and associated biogeochemical-ecological effects off the Jiangsu Shoal in the Western Yellow Sea, China. Journal of Geophysical Research: Oceans, 125(10): e2020JC016304, doi: 10.1029/2020JC016304
Wei Qinsheng, Li Xiansen, Wang Baodong, et al. 2016. Seasonally chemical hydrology and ecological responses in frontal zone of the central southern Yellow Sea. Journal of Sea Research, 112: 1–12
Wei Qinsheng, Wang Baodong, Yu Zhigang, et al. 2017. Mechanisms leading to the frequent occurrences of hypoxia and a preliminary analysis of the associated acidification off the Changjiang estuary in summer. Science China Earth: Sciences, 60(2): 360–381, doi: 10.1007/s11430-015-5542-8
Wei Qinsheng, Wang Baodong, Zhang Xuelei, et al. 2021a. Contribution of the offshore detached Changjiang (Yangtze River) Diluted Water to the formation of hypoxia in summer. Science of the Total Environment, 764: 142838, doi: 10.1016/j.scitotenv.2020.142838
Wei Qinsheng, Yao Peng, Xu Bochao, et al. 2021b. Coastal upwelling combined with the river plume regulates hypoxia in the Changjiang Estuary and adjacent inner East China Sea shelf. Journal of Geophysical Research: Oceans, 126(11): e2021JC017740, doi: 10.1029/2021JC017740
Woodson C B, Litvin S Y. 2015. Ocean fronts drive marine fishery production and biogeochemical cycling. Proceedings of the National Academy of Sciences of the United States of America, 112(6): 1710–1715
Wu Hui. 2015. Cross-shelf penetrating fronts: a response of buoyant coastal water to ambient pycnocline undulation. Journal of Geophysical Research: Oceans, 120(7): 5101–5119, doi: 10.1002/2014JC010686
Wu Hui, Shen Jian, Zhu Jianrong, et al. 2014. Characteristics of the Changjiang plume and its extension along the Jiangsu Coast. Continental Shelf Research, 76: 108–123, doi: 10.1016/j.csr.2014.01.007
Xu Jindian, Huang Jiang, Qiu Yun, et al. 2015. Spatial structure characteristics of Zhejiang and Fujian coastal water and their evolution. Journal of Tropical Oceanography (in Chinese), 34(1): 1–7
Xu Lingjing, Yang Dezhou, Benthuysen J A, et al. 2018. Key dynamical factors driving the Kuroshio Subsurface Water to reach the Zhejiang coastal area. Journal of Geophysical Research: Oceans, 123(12): 9061–9081
Xu Lingjing, Yang Dezhou, Greenwood J, et al. 2020. Riverine and oceanic nutrients govern different algal bloom domain near the Changjiang Estuary in summer. Journal of Geophysical Research: Biogeosciences, 125(10): e2020JG005727, doi: 10.1029/2020JG005727
Xuan Jiliang, Huang Daji, Pohlmann T, et al. 2017. Synoptic fluctuation of the Taiwan Warm Current in winter on the East China Sea shelf. Ocean Science, 13(1): 105–122, doi: 10.5194/os-13-105-2017
Yang Dezhou, Yin Baoshu, Liu Zhiliang, et al. 2012. Numerical study on the pattern and origins of Kuroshio branches in the bottom water of southern East China Sea in Summer. Journal of Geophysical Research: Oceans, 117(C2): C02014
Yang Dezhou, Yin Baoshu, Sun Junchuan, et al. 2013. Numerical study on the origins and the forcing mechanism of the phosphate in upwelling areas off the coast of Zhejiang province, China in Summer. Journal of Marine Systems, 123–124: 1–18
Ye Peng, Xuan Jiliang, Huang Daji. 2022. Evolution and dynamics of a summertime penetrating front off the Zhejiang-Fujian coast, China. Science China: Earth Sciences, 65(3): 556–569, doi: 10.1007/s11430-021-9853-x
Yuan Dongliang, Hsueh Y. 2010. Dynamics of the cross-shelf circulation in the Yellow and East China Seas in Winter. Deep-Sea Research Part II: Topical Studies in Oceanography, 57(19–20): 1745–1761, doi: 10.1016/j.dsr2.2010.04.002
Yuan Dongliang, Li Yao, He Lei, et al. 2010. An observation of the three-dimensional structure of a cross-shelf penetrating front off the Changjiang mouth. Deep-Sea Research Part II: Topical Studies Oceanography, 57(19–20): 1827–1834, doi: 10.1016/j.dsr2.2010.04.009
Yuan Dongliang, Qiao Fangli, Su Jie. 2005. Cross-shelf penetrating fronts off the southeast coast of China observed by MODIS. Geophysical Research Letters, 32(19): L19603
Zeng Dingyong, Ni Xiaobo, Huang Daji. 2012. Temporal and spatial variability of the Zhemin coastal current and the Taiwan warm current in winter in the southern Zhejiang coastal sea. Scientia Sinica (Terrae) (in Chinese), 42(7): 1123–1134, doi: 10.1360/zd-2012-42-7-1123
Zhao Linhong, Yang Dingtian, Zhong Rong, et al. 2022. Interannual, seasonal, and monthly variability of sea surface temperature fronts in offshore China from 1982–2021. Remote Sensing, 14(21): 5336
Zhou Silu, Wu Hui. 2023. Cross-shelf penetrating fronts of buoyant coastal currents around the headland. Journal of Geophysical Research: Oceans, 128(5): e2022JC019371, doi: 10.1029/2022JC019371
Zhou Feng, Xue Huijie, Huang Daji, et al. 2015. Cross-shelf exchange in the shelf of the East China Sea. Journal of Geophysical Research: Oceans, 120(3): 1545–1572, doi: 10.1002/2014JC010567
Zhu Zhuoyi, Wu Hui, Liu Sumei, et al. 2017. Hypoxia off the Changjiang (Yangtze River) estuary and in the adjacent East China Sea: quantitative approaches to estimating the tidal impact and nutrient regeneration. Marine Pollution Bulletin, 125(1–2): 103–114, doi: 10.1016/j.marpolbul.2017.07.029